

# Identification of machine tool geometric performance using on-machine inertial measurements

G.W. Vogl<sup>1</sup>, R. Pavel<sup>2</sup>, A. Archenti<sup>3</sup>, T.J. Winnard<sup>4</sup>, M.M. Mennu<sup>5</sup>, B.A Weiss<sup>1</sup>, and M.A. Donmez<sup>1</sup>

<sup>1</sup>National Institute of Standards and Technology (NIST), Gaithersburg, MD, USA

<sup>2</sup>TechSolve, Cincinnati, OH, USA

<sup>3</sup>KTH Royal Institute of Technology, Brinellvägen 68, 10044, Stockholm, Sweden

<sup>4</sup>Andrews University, Berrien Springs, MI, USA

<sup>5</sup>University of South Florida, Tampa, FL, USA

gvogl@nist.gov, pavel@TechSolve.org, archenti@kth.se, winnard@andrews.edu, mmennu@mail.usf.edu, brian.weiss@nist.gov, alkan.donmez@nist.gov

## Abstract

Machine tools degrade during operations, yet accurately detecting degradation of machine components such as linear axes is typically a manual and time-consuming process. Thus, manufacturers need automated and efficient methods to diagnose the condition of their machine tool linear axes with minimal disruptions to production. Towards this goal, a method was developed to use accelerometer and rate gyroscope data from an inertial measurement unit (IMU) for identification of changes in the translational and angular errors due to axis degradation. An IMU was created for application of the method on a machine tool. As a proof of concept for detection of translational error motions, IMU data was collected on a machine tool with experimentally simulated degradation; as the worktable moved along its nominal path, a cross-axis moved along a swept sinusoidal pattern with micrometer-level amplitudes. In another experiment, data was collected at three different locations on a worktable for the same axis motion. These experiments showed that the IMU detected micrometer-level and microradian-level degradation of linear axes, revealing that the IMU-based method is plausible for use in smart machine tools.

## Keywords

Machine tool, Linear Axis, Error, Degradation, Diagnostics

## 1. Introduction

Over a machine tool's lifetime, various faults lead to performance degradation, lowering accuracy and repeatability [1]. Typical sources of errors within linear axes are due to pitting, wear, corrosion, and cracks of the system components such as guideways and recirculating balls [2]. A typical machine tool has multiple linear axes, and their accuracies directly impact the quality of manufactured parts. As degradation increases, tool-to-workpiece errors increase that eventually may result in a loss of production quality and/or a failure [3]. Yet knowledge of degradation is elusive; proper assessment of axis degradation is often a manual, time-consuming, and potentially cost-prohibitive process.

While direct methods for machine tool performance evaluation are well-established [4] and reliable for position-dependent error quantification, such measurements typically interrupt production [5]. An online condition monitoring system for linear axes is needed to help reduce machine downtime, increase productivity and product quality, and improve knowledge about manufacturing processes [6]. Previous attempts at condition monitoring of linear axes had limited success, partly because of the lack of robustness and defined relationships of signals to axis

degradation composed of a wide range of spatial frequencies. Consequently, efficient quantitative measures are needed to monitor the degradation of linear axes.

## 2. IMU for Industrial Application

One potential solution for online monitoring of linear axis degradation is the use of an inertial measurement unit (IMU) [7, 8] that processes accelerometer and rate gyroscope data to detect changes in the translational and angular error motions due to axis degradation [8]. For industrial application, the IMU should be physically small and economical while satisfying measurement needs. As seen in Figure 1, an industrial IMU was created that is about 9 cm long and contains a triaxial accelerometer and a triaxial rate gyroscope. The bandwidths and noise properties of these sensors are shown in Table 1. A custom IMU was needed to satisfy design constraints such as cost, size, and accuracy.

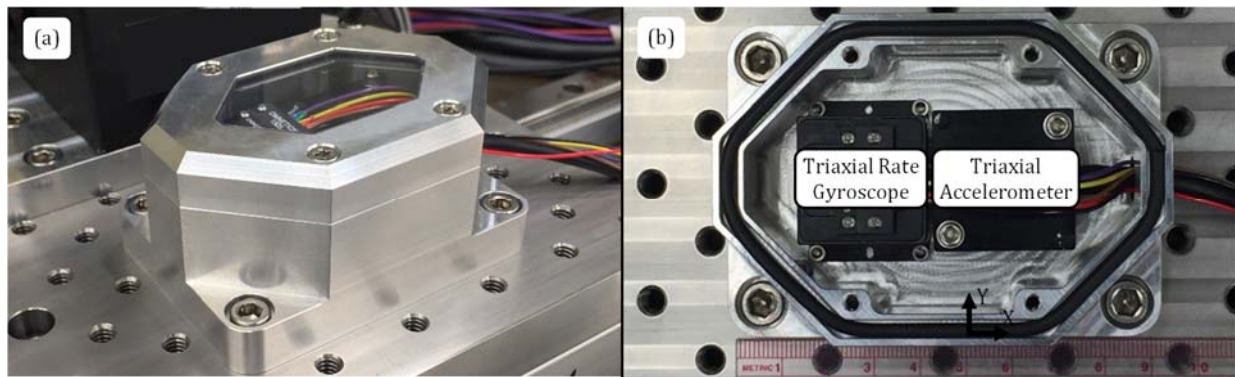


Figure 1 (a) Isometric view of industrial IMU and (b) top view of industrial IMU without its lid.

Table 1 Properties of sensors in industrial IMU.

Sensor	Bandwidth <sup>a</sup>	Noise
Accelerometer	0 Hz to 500 Hz	20 ( $\mu\text{m/s}^2$ )/ $\sqrt{\text{Hz}}$
Rate Gyroscope	0 Hz to 200 Hz	35 ( $\mu\text{rad/s}$ )/ $\sqrt{\text{Hz}}$

<sup>a</sup> frequencies correspond to half-power points, also known as 3 dB points

## 3. Detection of Translational Degradation

Repeated testing of the IMU on a machine tool is required for acceptance testing. Figure 2 shows an experimental setup of the IMU on a horizontal milling machine at TechSolve, Inc. The IMU is attached to the worktable, which can translate in two directions since the X-axis is stacked on the Z-axis. Of course, unwanted translational errors exist and can worsen due to degradation as the machine tool produces parts. For example, the error motion  $E_{ZX}$  is the translational error, as a function of X, in the Z-direction for X-axis motion. Because the X- and Z-axes are stacked for the machine tool, we can simulate  $E_{ZX}$  via two-axis commanded motion. The boxed inset of Figure 2 shows the points used for machine path generation. As the X-axis moves from 0 mm to 1250 mm, the Z-axis experiences a swept-sine-like form of degradation with magnitude  $A$ . The path is independent of feed rate, which can be as large as 10 m/min (0.1667 m/s). Hence, data was collected for 50 runs for each of three speeds for use within the method [8]: 0.1667 m/s (Fast speed), 0.1 m/s (Moderate speed), and 0.02 m/s (Slow speed). The fast speed of 0.1667 m/s was the machine limit, but preferably a speed of 0.5 m/s would have been used otherwise. Furthermore,

the magnitude  $A$  was changed to represent different levels of degradation. Data was collected for five values of  $A$ :  $0\ \mu\text{m}$  (representing no degradation),  $5\ \mu\text{m}$ ,  $10\ \mu\text{m}$ ,  $15\ \mu\text{m}$ , and  $20\ \mu\text{m}$  (representing significant degradation). Consequently, the swept-sine-like motion is a “mechanically-simulated degradation” that will test the ability of the industrial IMU to measure micrometer-level degradation for various spatial frequencies.

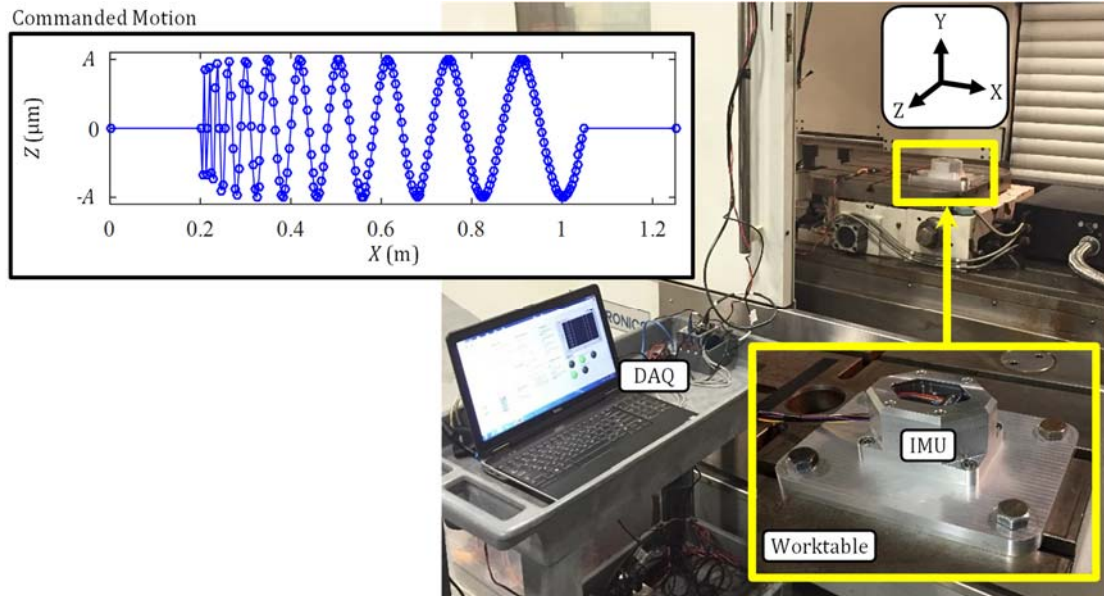


Figure 2 Experimental setup of IMU on machine tool at TechSolve. Commanded machine tool motion ( $Z$  versus  $X$ ) shown in boxed inset.

IMU data was collected and processed for each of the five values of  $A$ , the parameter representing translational error motion in the  $Z$ -direction due to ‘degradation’. The results of each set of 50 runs were averaged to yield the estimated straightness error motion  $E_{ZX}$  for each value of  $A$ . Figure 3(a) and Figure 3(b) compare the commanded and estimated values for  $hp(E_{ZX})$ , the high-pass filtered values of  $E_{ZX}$ . The error motions are high-pass filtered because the specific accelerometer was determined *post facto* to have noise during testing that exceeded the noise specification listed in Table 1. Hence, convergence of  $E_{ZX}$  did not occur to sufficient levels for spatial frequencies below  $1.25\ \text{m}^{-1}$ , so those terms were filtered out via the use of zero-phase forward and reverse digital infinite impulse response (IIR) Butterworth filters.

Figure 3(b) shows how the mechanically-simulated degradation is detected by the IMU-based method. As the commanded degradation amplitude  $A$  increases to  $20\ \mu\text{m}$ , as seen in Figure 3(a), the estimated degradation amplitude also increases, as shown in Figure 3(b). Error motions due to the sensor noise and mechanical elements of the machine tool are present in the curves of Figure 3(b), but the degradation terms are still clearly visible. The estimated degradation amplitudes seen in Figure 3(b) are roughly similar to the commanded ones seen in Figure 3(a), but the estimated amplitudes increase as the spatial frequency of the swept-sine decreases. When the spatial frequency is at its highest around  $X = 0.2\ \text{m}$ , the required accelerations for the commanded motions within Figure 3(a) for  $A = 20\ \mu\text{m}$  are as high as  $1.75\ \text{m/s}^2$  for the fast speed ( $0.1667\ \text{m/s}$ ), which is far greater than the maximum allowable acceleration for the machine tool during feed motion. Hence, the high-frequency motions for  $A = 20\ \mu\text{m}$  near  $X = 0.2\ \text{m}$  are not detectable

because they did not occur with amplitudes near 20  $\mu\text{m}$ , but rather with much smaller amplitudes. Unfortunately, a laser-based device, such as a laser tracker, was not available to measure the actual amplitudes during motion for verification and validation of the acceleration-limiting motion.

The high-passed motions, shown in Figure 3 for various amplitudes  $A$ , can be processed with a single metric value for comparison and tracking of ‘degradation’. Figure 3(c) shows the scaled root mean square (rms) of each of the curves seen in Figure 3(a) and Figure 3(b). The metric for the commanded motion increases linearly from 0  $\mu\text{m}$  (the smallest value for  $A$ ) to 20  $\mu\text{m}$  (the largest value for  $A$ ) as  $A$  increases, while the metric for the estimated motion increases fairly linearly from about 5  $\mu\text{m}$  to about 16  $\mu\text{m}$ . The estimated-motion metric value reaches 5  $\mu\text{m}$ , instead of 0  $\mu\text{m}$ , at  $A = 0 \mu\text{m}$  because even with no commanded cross-axis motion ( $A = 0 \mu\text{m}$ ), the Z-axis still exhibits an error motion as the X-axis moves. At the other end, the estimated-motion metric value reaches 16  $\mu\text{m}$ , instead of 20  $\mu\text{m}$ , at  $A = 20 \mu\text{m}$  because of the machine tool’s acceleration limit that inhibits the Z-axis motion, as evidenced in Figure 3(b). Nonetheless, Figure 3(c) reveals how even a simple metric, based on results from the IMU-based method, can track linear axis degradation in a quantitative manner.

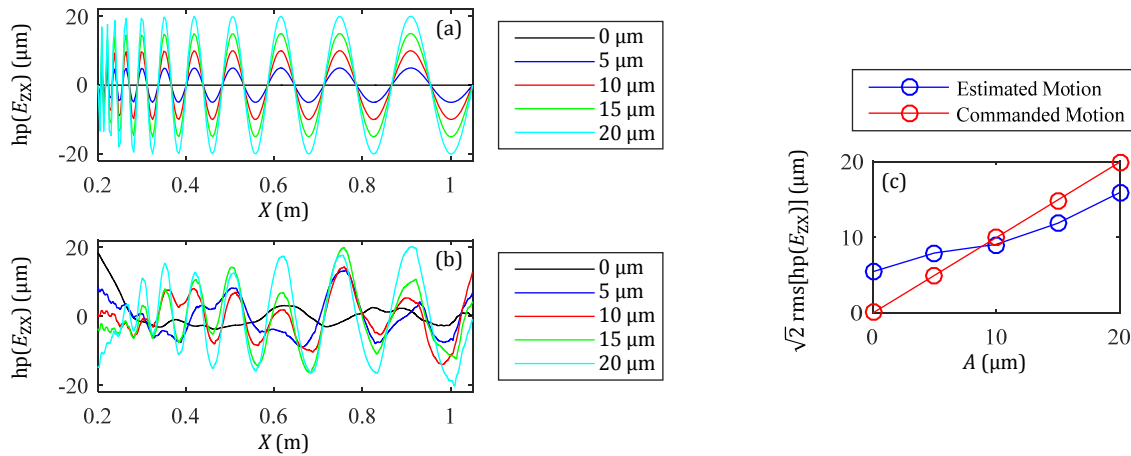


Figure 3 Comparison of (a) commanded and (b) estimated high-pass filtered error motions with their (c) metric values as a function of ‘degradation’ amplitude.

#### 4. Detection of Angular Error Motion

Another experiment was conducted to test the capability of the IMU for on-machine detection of error motions. However, before experimentation, the IMU was improved via replacement of the triaxial accelerometer with a different model that had relatively stable low-frequency noise, but higher overall noise ( $69 (\mu\text{m}/\text{s}^2)/\sqrt{\text{Hz}}$ ) compared to the accelerometer used in the first experiment (see Table 1).

Figure 4(a-d) shows an experimental setup of the IMU on a vertical milling machine at the National Institute of Standards and Technology (NIST). For each dataset, the IMU is attached to the worktable at one of three different locations (A, B, or C) and the Y-axis travels between  $Y = 0 \text{ m}$  and  $Y = 0.5 \text{ m}$ . Hence, IMU data was collected for 50 runs sequentially at each location with motion back and forth along the Y axis for use within the method [8]. The three speeds for data collection are 0.5  $\text{m/s}$  (fast speed), 0.1  $\text{m/s}$  (moderate speed), and 0.02  $\text{m/s}$  (slow speed). The IMU data was then used to estimate the three angular error motions at each of the three worktable locations (A, B, and C). The accelerometer and rate gyroscope data were processed to estimate

two angular error motions ( $E_{AY}$  and  $E_{BY}$ ) according to Fig. 3(b) in Ref. [8], while the rate gyroscope data only was used to estimate the third angular error motion ( $E_{CY}$ ) according to Fig. 3(a) in Ref. [8]. If the worktable is rigid, then the estimated angular error motions should be identical among each location.

Figure 4(e-g) shows the estimated angular errors based on the IMU data. Error motion data was also collected at each location with a laser-based commercial reference system (with standard uncertainties of  $0.7 \mu\text{m}$  and  $3.0 \mu\text{rad}$ ), and the data from the reference system is shown in the figures (as thinner lines) for comparison purposes. At each worktable location, reference data was collected for five runs, which were averaged to produce the curves seen in Figure 4(e-g). The standard deviations of each set of five runs was also used to produce the shaded 95%-confidence zones in Figure 4(e-g). Thus, the shaded zones represent a contribution towards, but not the total of, the measurement uncertainty. As seen in Figure 4(e-g), the estimated angular errors from the IMU data match each other respectively to within about  $5 \mu\text{rad}$  for the three worktable locations (A, B, and C). Also, the estimated error motions from the IMU match those from the reference system to within about  $8 \mu\text{rad}$ . The differences may be due to differences in error type (inertial for IMU, while relative for the reference system) as well as to sources of uncertainty.

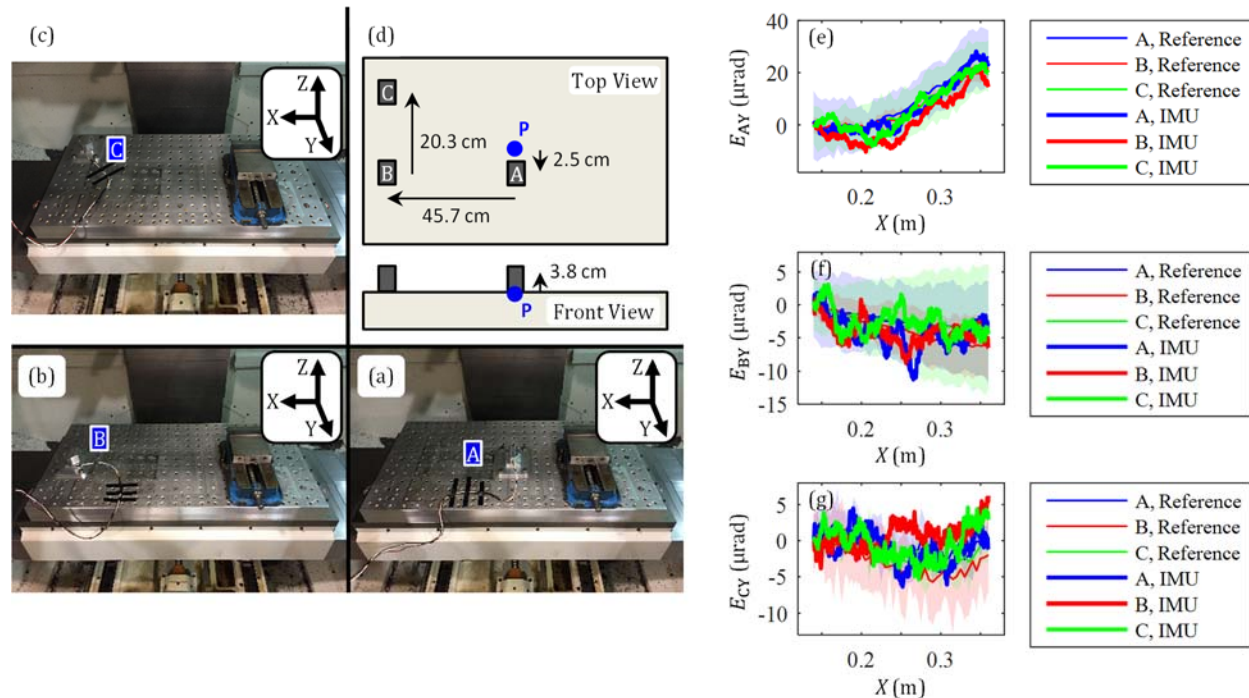


Figure 4 Experimental setup of IMU on machine tool worktable: Pictures of IMU at (a) Location A, (b) Location B, and (c) Location C and (d) schematic of three IMU locations relative to center point P of worktable. Angular errors (e)  $E_{AY}$ , (f)  $E_{BY}$ , and (g)  $E_{CY}$  based on data collected at the three locations (Locations A, B, and C) with the IMU and a commercial reference system. The reference data has shaded areas representing measurement expanded uncertainties ( $k = 2$ ) at 95% confidence based on five runs.

## 5. Conclusions

An ‘industrial IMU’ was developed to test the effectiveness of a new IMU-based method for on-machine application. The industrial IMU includes a triaxial accelerometer and a triaxial rate gyroscope, both with noise levels shown to be sufficiently low for convergence via averaging. One

experiment was conducted in which two stacked axes were moved simultaneously to simulate translational degradation up to 20  $\mu\text{m}$  in amplitude. The IMU data showed that the mechanically-simulated degradation is detected by the IMU-based method. However, the error motions needed to be high-pass filtered because the specific accelerometer had noise levels that exceeded its specification, revealing how the industrial IMU must be improved for future applications. In a second experiment, data was collected from an improved IMU at three different locations on a worktable for the same axis motion. The IMU results were within about 8  $\mu\text{rad}$  of those from a laser-based reference system. Both experiments show that the IMU-based method is capable of detecting micrometer-level and microradian-level degradation of linear axes.

When coupled with existing data exchange and formatting standards, verified and validated data from an ‘industrial IMU’ could provide manufacturers and machine tool operators with near-real-time equipment health, diagnostic, and prognostic intelligence to significantly enhance asset availability and minimize unscheduled maintenance. This information can be coupled with equipment performance metrics and quality data (resultant from part inspection) to enable the prediction of future machine performance and part quality based upon current and projected equipment health.

### Acknowledgements

The authors thank Brian Pries, Travis Shatzley, Dan Falvey, and Jay Brandenburg of the Fabrication Technology Group (NIST), and Dennis Dill (TechSolve) for their outstanding contributions with the experimental setup.

### References

- [1] Li Y, Wang X, Lin J, Shi S (2014) A Wavelet Bicoherence-Based Quadratic Nonlinearity Feature for Translational Axis Condition Monitoring. *Sensors* 14(2):2071-2088.
- [2] Zhou Y, Mei X, Zhang Y, Jiang G, Sun N (2009) Current-Based Feed Axis Condition Monitoring and Fault Diagnosis. *4th IEEE Conference on Industrial Electronics and Applications, ICIEA 2009*, 1191-1195.
- [3] Uhlmann E, Geisert C, Hohwieler E (2008) Monitoring of Slowly Progressing Deterioration of Computer Numerical Control Machine Axes. *Proceedings of the Institution of Mechanical Engineers, Part B: Journal of Engineering Manufacture* 222(10):1213-1219.
- [4] International Organization for Standardization (2012) ISO 230-1 - Test Code for Machine Tools – Part 1: Geometric Accuracy of Machines Operating under No-Load or Quasi-Static Conditions.
- [5] Khan AW, Chen W (2009) Calibration of CNC Milling Machine by Direct Method. *2008 International Conference on Optical Instruments and Technology: Optoelectronic Measurement Technology and Applications*, 7160:716010.
- [6] Teti R, Jemielniak K, O'Donnell G, Dornfeld D (2010) Advanced Monitoring of Machining Operations. *CIRP Annals - Manufacturing Technology* 59(2):717-739.
- [7] Vogl GW, Weiss BA, Donmez MA, 2015, A Sensor-Based Method for Diagnostics of Machine Tool Linear Axes, Annual Conference of the Prognostics and Health Management Society 2015. Coronado, CA: PHM Society, p. 10.
- [8] Vogl GW, Donmez MA, Archenti A (2016) Diagnostics for Geometric Performance of Machine Tool Linear Axes. *CIRP Annals - Manufacturing Technology*